Journal of Industrial Pollution and Toxicity
Volume 1 | Issue 1

Research Article Open Access

On Similarity of Pressure Head and Bubble Pressure Fractal Dimensions for Characterizing Permo-Carboniferous Shajara Formation, Saudi Arabia

Al-Khidir KE*

Department of Petroleum and Natural Gas Engineering, College of Engineering, King Saud University, Saudi Arabia

***Corresponding author:** Al-Khidir KE, Ph.D, Department of Petroleum and Natural Gas Engineering, College of Engineering, King Saud University, Saudi Arabia, E-mail: kalkhidir@ksu.edu.sa

Citation: Al-Khidir KE (2018) On Similarity of Pressure Head and Bubble Pressure Fractal Dimensions for Characterizing Permo-Carboniferous Shajara Formation, Saudi Arabia. J Indust Pollut Toxic 1(1): 102

Abstract

Pressure head was gained from distribution of pores to characterize the sandstones of the Shajara reservoirs of the permo-Carboniferous Shajara Formation. The attained values of pressure head was employed to calculate the pressure head fractal dimension. Based on field observations in addition to the acquired values of pressure head fractal dimension, the sandstones of Shajara reservoirs were divided here into three units. The obtained units from base to top are: Lower Shajara Pressure Head Fractal Dimension Unit, Middle Shajara Pressure Head Fractal Dimension Unit and Upper Shajara Pressure Head Fractal Dimension Unit.

The three Shajara reservoirs were also confirmed by the ratio of bubble pressure to capillary pressure at other points versus effective saturation. It was reported that the permeability accelerates with increasing bubble pressure fractal dimension due to the naturally occurring interconnected channels. The pressure head fractal dimension and bubble pressure fractal dimension was successfully characterize the sandstones of the Shajara reservoirs with certain degree of accuracy.

Keywords: Permo-Carboniferous, head fractal dimension

Introduction

Capillary pressure is generally expressed as an aspect of the wetting phase saturation, according to the capillary pressure model [1]. The capillary pressure function was modified by Brooks and Corey (1964) by applying a pore size distribution index (λ) as an exponent on the ratio of bubble pressure to capillary pressure [2]. According to their results, a linear relationship exists between pres¬sure and effective saturation on a log-log plot. This mathematical relationship has been named the Brooks-Corey model (B-C mod¬el). A model that predicts the hydraulic conductivity for un- satu¬rated soil-water retention curve and conductivity saturation was derived by Mualem (1976) [3]. Later, based on Mualem's formula, Van Genuchten (1980) described a relatively simple expression for the hydraulic conductivity of unsaturated soils [4]. The Van Genu¬chten model (V-G model) contained three independent parameters, which can be obtained by fitting experimental data. A function to estimate the relationship between water saturation and capillary pressure in porous media was proposed by Oostrom and Len¬hard (1998) [5]. This function is test data of sandstone rocks and carbonate rocks with high permeability were described by a new capillary pressure expression by Jing and Van Wunnik (1998) [6].

A fractal approach can be used to model the pc measured with mercury intrusion in Geysers grey wackerock; however, the B-C model could not be used, according to a study by Li (2004) [7]. Sub-sequently, a theoretical analysis using fractal geometry was conducted by Li and Horne (2006) to deduce the B-C model, which has always been considered as an empirical model [8]. Subsequently, fractal modeling of porous media was used to de¬velop a more generalized capillary pressure model (Li, 2010a) [9]. With the new model, he also evaluated the heterogeneity of rocks (Li, 2010b) [10]. Al-Khidir, *et al.* 2011 studied Bimodal Pore Size behavior of the Shajara Formation reservoirs of the permo-carboniferous Unayzah group [11]. Al-Khidir, *et al.* (2012) sub¬divided the Shajara reservoirs into three units based on thermody¬namic fractal dimension approach and 3-D fractal geometry model of mercury intrusion technique [12]. The work published by Al-Khidir, *et al.* 2012 was cited as Geoscience; New Finding reported from King Saud University Describe advances in Geoscience. Science Letter (Oct 25, 2013): 359. Al-khidir, *et al.* 2013 subdivide the Shajara reservoirs into three units: Lower Shajara Differen¬tial Capacity Fractal Dimension Unit, Middle Shajara Differential Capacity Fractal Dimension Unit, Upper Shajara Differential Ca¬pacity Fractal Dimension Unit [13,14]. The Three reservoirs units were confirmed by water saturation fractal dimension. Al-Khidir 2015 subdivided the Shajara reservoirs into three induced

polariza-tion geometric time fractal dimension units and confirmed them by arithmetic relaxation time fractal dimension of induced polariza¬tion [15]. Similarity of geometric and arithmetic relaxation time of induced polarization fractal dimensions was reported by Al-khidir [2018].

The purpose of this paper is to obtain pressure head fractal dimension (Dαh) and to confirm it by bubble pressure fractal dimension (DP/pc). The pressure head fractal dimension is determined from the slope of the plot of effective wetting phase saturation (log Se) versus log pressure head (α*h). The exponent on the pressure head relates to the fitting parameters m*n which match with the pore size distribution index (λ). The bubble pressure fractal dimension was obtained from the slope of the plot of wetting phase

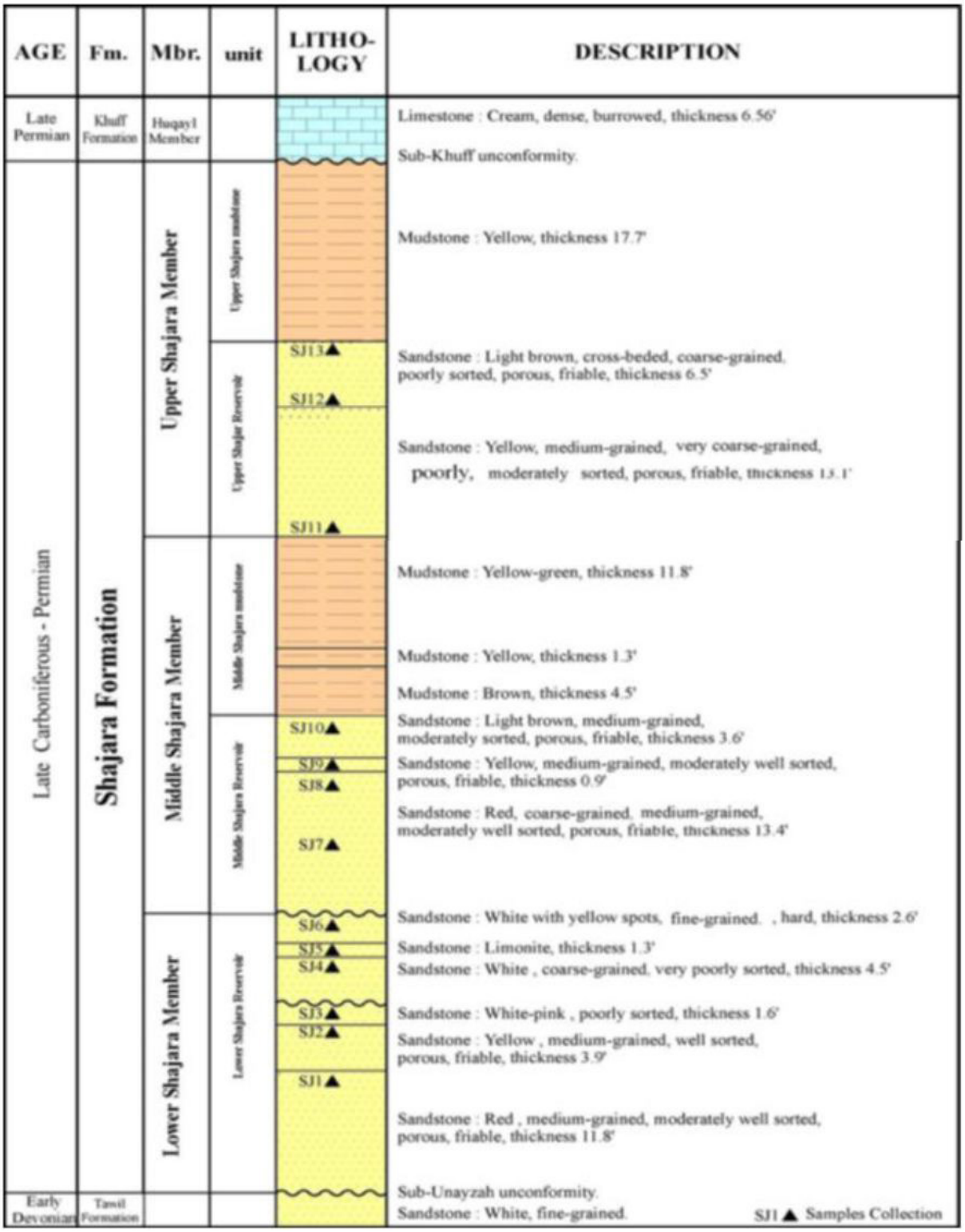

Figure 1: Stratigraphic column of the type section of the Permo-Carboniferous Shajara Formation, Wadi Shajara, Qusayba area, al Qassim district, Saudi Arabia, Latitude 26° 52' 17.4", longitude 43° 36' 18. "

effect tive saturation (log Se) versus the plot of the log of ratio of bubbling pressure (Pb) to capillary pressure (pc). The slope of the functional relationships among capillary pressure and effective saturation correspond to the pore size distribution index (λ). Theoretically, the pore size distribution index being small for media having a wide range of pore sizes and large for media with a relatively uniform pore size. Sandstone samples were collected from the surface type section of the Permo-Carboniferous Shajara Formation, Wadi Shajara, Qusayba area, al Qassim district, Saudi Arabia, N 26 52 17.4, E 43 36 18 (Figure1). Porosity was measured on collected samples using mercury intrusion Porosimetry and permeability was derived from capillary pressure data.

Mathematical and theoretical aspects

The pressure head can be scaled as

$$Se = \left(\alpha * h\right)^{-m*n} \tag{1}$$

Where Se = effective wetting phase saturation.
α = inverse of entry capillary pressure head in cm-1.
h = capillary pressure head in cm.
m * n soil characteristics parameter (fitting parameters).
Equation 1 can be proofed from number of pores theory. Based on number of pores theory, the pore throat radius is scaled as follows:

$$N\left(r\right) \propto r^{-Df} \tag{2}$$

Where N(r) number of pores; r pore throat radius and Df is the fractal dimension. The number of pores can be defined as the ratio of volume to the volume of the unit cell. If we consider the unit cell as sphere, then the number of pores is defined as:

$$N\left(r\right) = \frac{v}{\frac{4}{3} * \pi * r^3} \tag{3}$$

Insert equation 2 into equation 3

$$v \propto r^{3-Df} \tag{4}$$

The pore throat radius (r) is defined as follows:

$$r = \frac{2 * \sigma * \cos\theta}{p_c} \tag{5}$$

Where σ is the surface tension of mercury 485 dyne /cm, θmercury contact angle 130°, p_c is the capillary pressure.

Insert equation 5 into equation 4

$$v \propto P_c^{-\left(3-Df\right)} \tag{6}$$

Differentiate equation 6 with respect to pc

$$\frac{dv}{dP_c} \propto P_c^{(Df-4)} \tag{7}$$

If we remove the proportionality sign of equation 7 we have to multiply by a constant

$$\frac{dv}{dP_c} = con\tan t * P_c^{Df-4} \tag{8}$$

Integrate equation 8 will result in

$$\int dv = cons\tan t \int_{P_{c\min}}^{P_c} P_c^{Df-4} * dP_c \tag{9}$$

$$v = \frac{cons\tan t}{Df-3} * \left[pc^{Df-3} - Pc_{\min}^{Df-3} \right] \tag{10}$$

The integration of the total volume will give

$$\int dv\,total = cons\tan t \int_{Pc_{\min}^{Df-3}}^{Pc_{\max}^{Df-3}} pc^{Df-4} * dpc \tag{11}$$

$$\mathbf{vtotal} = \frac{\mathbf{constant}}{\mathbf{Df}-3} * \left[\mathbf{Pc_{max}^{Df-3}} - \mathbf{Pc_{min}^{Df-3}} \right] \tag{12}$$

If we divide equation 10 by equation 12 we can obtain the effective wetting phase saturation

$$se = \frac{v}{vtotat} = \frac{\left[\frac{\mathbf{constant}}{\mathbf{Df}-3} * \left[\mathbf{pc^{Df-3}} - \mathbf{Pc_{min}^{Df-3}} \right] \right]}{\left[\frac{\mathbf{constant}}{\mathbf{Df}-3} * \left[\mathbf{Pc_{max}^{Df-3}} - \mathbf{Pc_{min}^{Df-3}} \right] \right]} \tag{13}$$

$P_{cmin} << p_c$ then equation 13 after simplification will result in

$$se = \frac{\mathbf{pc^{Df-3}}}{\mathbf{pcmax^{Df-3}}} \tag{14}$$

If pressure head (h) is used instead of capillary pressure (pc) and maximum capillary pressure (p_{cmax}) is replaced by entry capillary pressure head (he) equation 14 will become

$$\mathbf{Se} = \frac{\mathbf{h^{Df-3}}}{\mathbf{he^{Df-3}}} \tag{15}$$

$$\text{But, } \frac{1}{he} = \alpha = \text{ inverse of entry capillary presssurehead} \tag{16}$$

Insert α into equation 15

$$Se = \left(\alpha * h\right)^{Df-3} = (\alpha * h)^{-\lambda} = (\alpha * h)^{-m*n} \tag{17}$$

Equation 17 is the proof of 1.

Results

The obtained results of the log log plot of the ratio of bubble pressure (Pb) to pressure (pc) and the product of inverse pressure head (α) and pressure head (h) versus effective wetting phase satu¬ration (Se) are shown in (Figures 2 and 11). A straight line was attained whose slope is equal to the pore size distribution index (λ) of Brooks and Corey (1964) and the fitting parameters m times n of Van Genuchten (1980) respectively [2,4]. Based on the acquired results it was found that the pore size distribution index

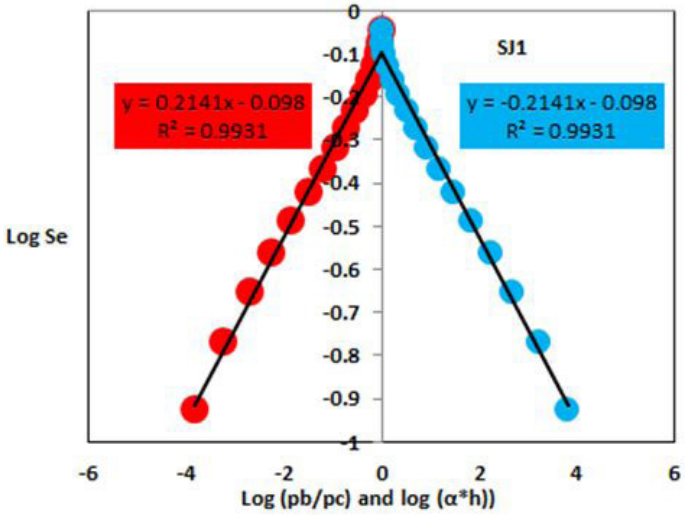

Figure 2: Log (Pb/pc) versus log Se in red color and Log (α*h) versus log Se in blue Color for sample SJ1

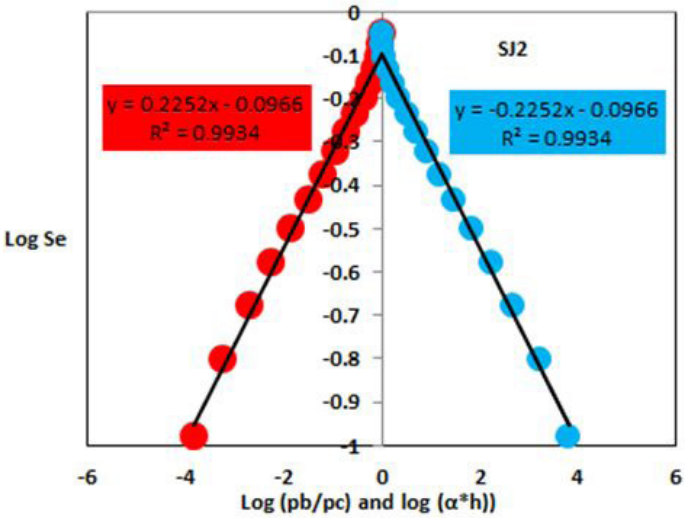

Figure 3: Log (Pb/pc) versus log Se in red color and Log (α*h) versus log Se in blue Color for sampleSJ2

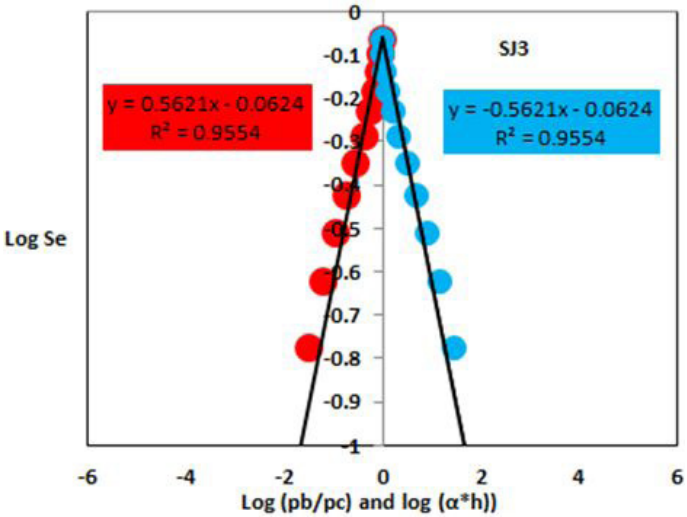

Figure 4: Log (Pb/pc) versus log Se in red color and Log (α*h) versus log Se in blue Color for sample SJ3

is equal to the fitting parameters m*n. The maximum value of the pore size distribution index was found to be 0.4761 assigned to sample SJ5 from the Lower Shajara Reservoir (Table 1). Whereas the minimum value of the pore size distribution index was reported from sample SJ13 from the Upper Shajara reservoir (Table 1). The pore size distribution index and the fitting parameters m*n were observed to decrease with increasing permeability owing to the possibility of having interconnected channels (Table 1). The bubble pressure fractal dimension and pressure head fractal dimension which were derived from the pore size index were noticed to in¬crease with increasing permeability and show similarity in their values (Table 1). Based on field observation the Shajara Reservoirs of the Permo-Carboniferous Shajara Formation were divided into three units (Figure 1).

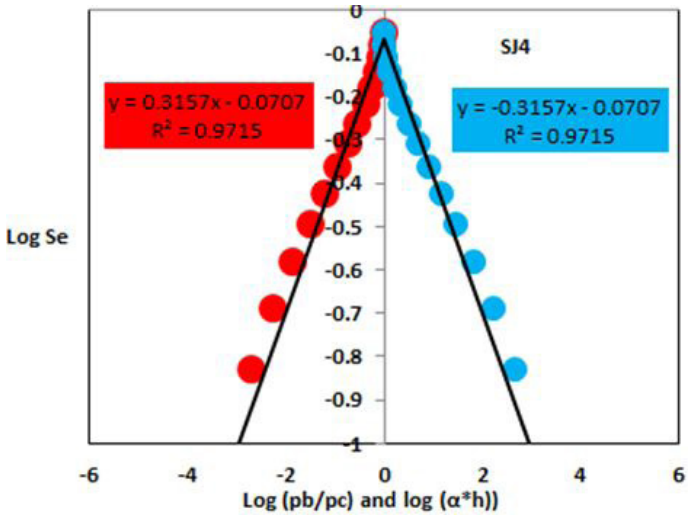

Figure 5: Log (Pb/pc) versus log Se in red color and Log (α*h) versus log Se in blue Color for sample SJ4

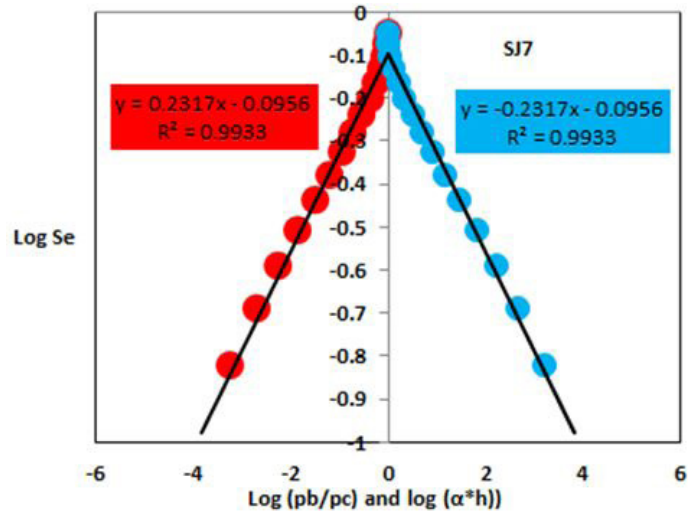

Figure 6: Log (Pb/pc) versus log Se in red color and Log (α*h) versus log Se in blue Color for sample SJ7

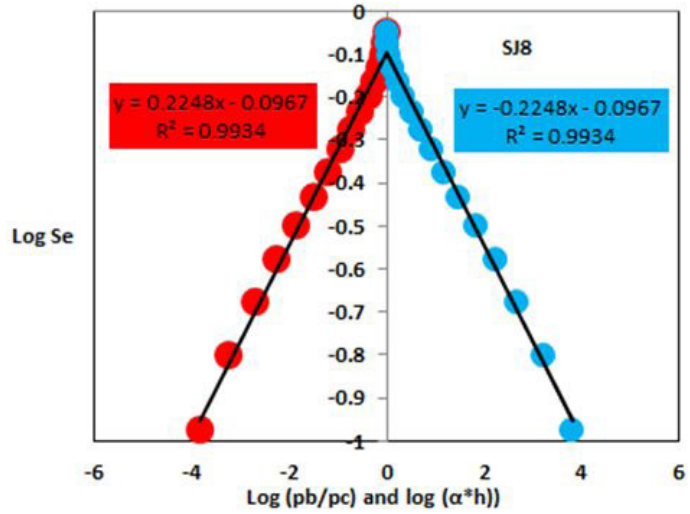

Figure 7: Log (Pb/pc) versus log Se in red color and Log (α*h) versus log Se in blue Color for sample SJ8

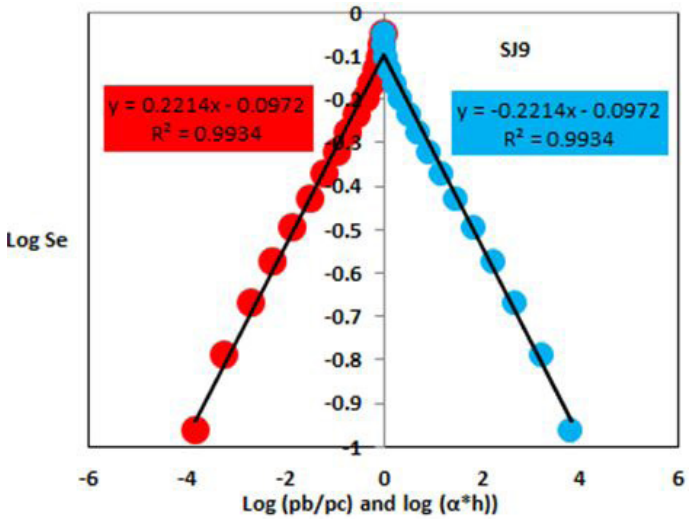

Figure 8: Log (Pb/pc) versus log Se in red color and Log (α*h) versus log Se in blue Color for sample SJ9

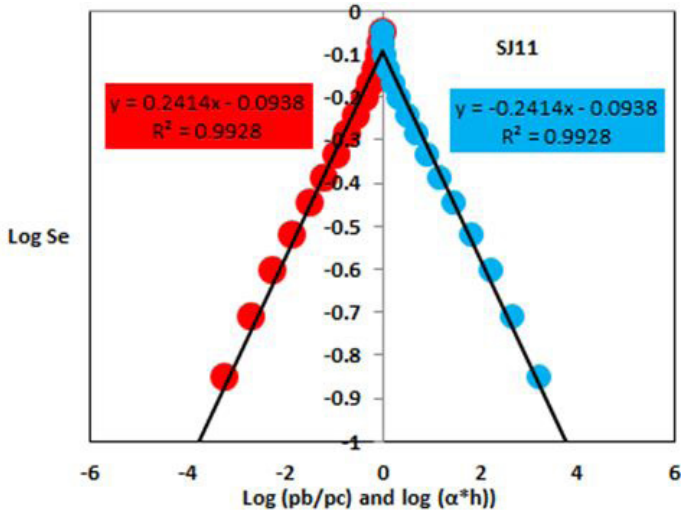

Figure 9: Log (Pb/pc) versus log Se in red color and Log (α*h) versus log Se in blue Color for sample SJ11

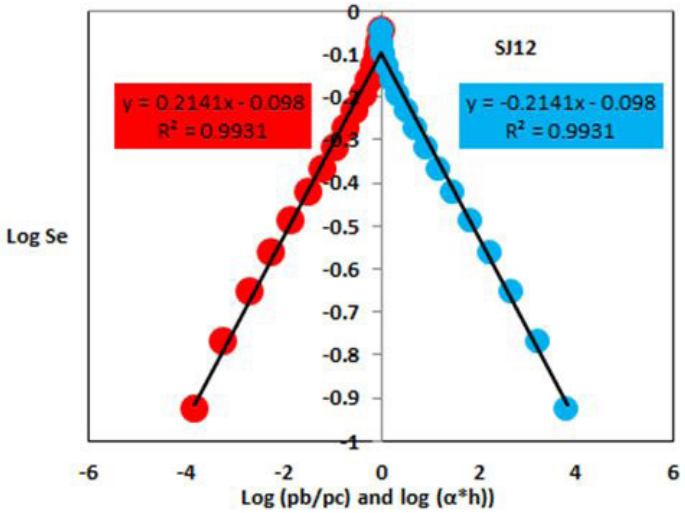

Figure 10: Log (Pb/pc) versus log Se in red color and Log (α*h) versus log Se in blue Color for sample SJ12

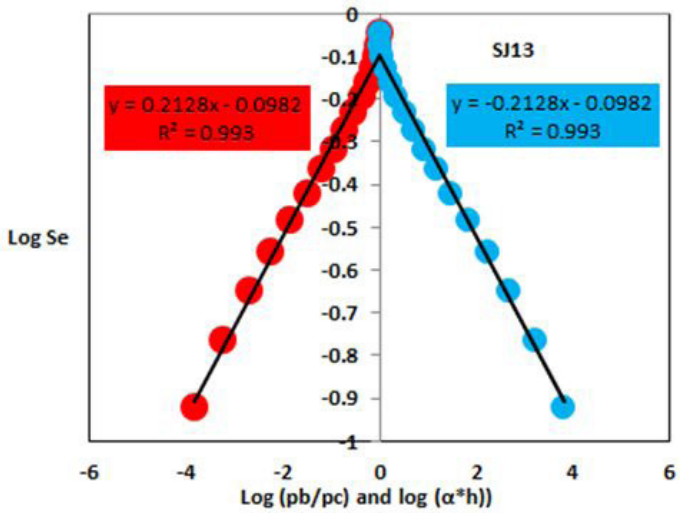

Figure 11: Log (Pb/pc) versus log Se in red color and Log (α*h) versus log Se in blue Color for sample Sj13

Formation	Reservoir	Sample	Φ %	K (md)	λ	m*n	m	n	Dp/pc	Dαh
Permo Carboniferous Shajara Formation	Lower Shajara Reservoir	SJ1	29	1680	0.2141	0.2141	0.176345	1.2141	2.7859	2.7859
		SJ2	35	1955	0.2252	0.2252	0.183807	1.2252	2.7748	2.7748
		SJ3	34	56	0.5621	0.5621	0.359836	1.5621	2.4379	2.4379
		SJ4	30	176	0.3157	0.3157	0.239948	1.3157	2.6843	2.6843
	Middle Shajara Reservoir	SJ7	35	1472	0.2317	0.2317	0.188114	1.2317	2.7683	2.7683
		SJ8	32	1344	0.2248	0.2248	0.18354	1.2248	2.7752	2.7752
		SJ9	31	1394	0.2214	0.2214	0.181267	1.2214	2.7786	2.7786
	Upper Shajara Reservoir	SJ11	36	1197	0.2414	0.2414	0.194458	1.2414	2.7586	2.7586
		SJ12	28	1440	0.2141	0.2141	0.176345	1.2141	2.7859	2.7859
		SJ13	25	973	0.2128	0.2128	0.175462	1.2128	2.7872	2.7872

Table 1: Petrophysical properties characterizing Shajara reservoirs of the Permo-Carboniferous Shajara Formation

These units from base to top are: Lower Shajara Reservoir, Middle Shajara reservoir, and Upper Shajara Reservoir. The Lower Shajara reservoir was represented by four sandstone samples out of six, namely SJ1, SJ2, SJ3 and SJ4. Sample SJ1 is described as medium-grained, porous, permeable, and moderately well sorted red sandstone (Figure 1). Its pore size distribution index and fitting parameter m*n show similar values (Figure 2) (Table 1). Its bubble pressure fractal dimension and pressure head fractal dimension which was derived from pore size distribution index and the fitting parameter m*n respectively also indicates similar values (Table 1). delineates straight line plot of log (Pb/pc) versus log effective saturation, and log (α*h) versus log effective saturation of sample SJ2 which is defined as medium - grained, porous, permeable, well sorted, yellow sandstone (Figure 1 and 3). It acquired a pore size distribution index of about 0.2252 whose value equal to m*n (Figure 3). It is also characterized by similarity in bubble pressure frac¬tal dimension and pressure head fractal dimension as displayed in Table 1. As we proceed from sample SJ2 to SJ3 a pronounced re¬duction in permeability due to compaction was reported from 1955 md to 56 md which reflects an increase in pore size distribution index from0.2252 to 0.5621 and reduction in fractal dimension from 2.7748 to 2.4379 as stated in (Table 1). Again, an increase in grain size and permeability was recorded from sample SJ4 which is characterized by 0.3157 pore size distribution index and 2.6843 bubble pressure fractal dimension which agree with the pressure head fractal dimension (Table 1).

In contrast, the Middle Shajara reservoir which is separated from the Lower Shajara reservoir by an unconformity surface was designated by three sam¬ples out of four, namely SJ7, SJ8, and SJ9 as illustrated in Figure 1. Their pore size distribution index and fitting parameters m*n were reported in Figures 5,6,7, 8 (Table 1). Their bubble pressure fractal dimensions and pressure head fractal dimensions are higher than those of samples SJ3 and SJ4 from the Lower Shajara Reservoir due to an increase in their per¬meability (Table 1).

On the other hand, the Upper Shajara reservoir is separated from the Middle Shajara reservoir by yellow green mudstone as demonstrated in Figure 1. It is defined by three sam¬ples so called SJ11, SJ12, SJ13 as explained in Figure 1. Further¬more, their pore size distribution index and the fitting parameters m*n were demonstrated in Figure 9,10 and 11 (Table 1). Moreover, their bubble pressure fractal dimension and pres-sure head fractal dimension are also higher than those of sample SJ3 and SJ4 from the Lower Shajara Reservoir due to an increase in their flow capacity (permeability) as explained in (Table 1).

Overall a plot of pore size distribution index and the fitting param¬eter param¬eter n versus fractal dimension reveals three perme¬able zones of varying Petrophysical properties (Figure 12). The higher fractal dimension zone with fractal dimension higher than 2.75 corresponds to the full Upper Shajara Reservoir, entire Middle Shajara Reservoir and Sample SJ1 and SJ2 from the lower Shajara Reservoir (Figure 12). The middle fractal dimension zone with a value of about 2.68 resembles sample SJ4 from the lower Shajara res¬ervoir (Figure 12). The lower fractal dimension value 2.43 allocates to sample SJ3 from the Lower Shajara reservoir as shown in Figure 12. The three Shajara fractal dimension zones were also confirmed by plot¬ting pressure head fractal dimension versus bubble pressure fractal dimension as illustrated in Figure 13.

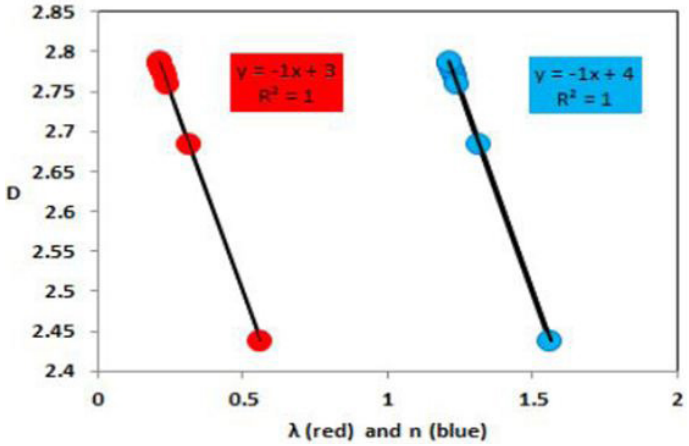

Figure 12: Pore size distribution index (λ) in red color and fitting param¬eter (n) in blue color versus fractal Dimension (D).

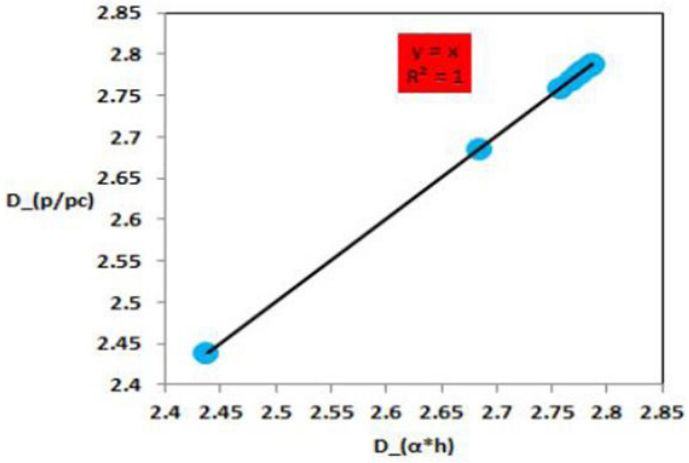

Figure 13: Pressure head fractal dimension (Dαh) versus bubble pressure fractal dimension (DP/pc).

Conclusion

The obtained Shajara bubble pressure fractal dimension reservoir units were also confirmed by pressure head fractal dimension. It was found that, the higher the bubble pressure fractal dimension and pressure head fractal dimension, the higher the permeability leading to better Shajara reservoir characteristics. It was also reported that, the bubble pressure fractal dimension and pressure head fractal dimension increases with decreasing pore size distribution index and fitting parameters m*n owing to possibility of having interconnected channels. Digenetic features such as compaction plays an important role in reducing bubble pressure fractal dimension and pressure head fractal dimension due to reduction in pore connectivity.

Acknowledgement

The author would like to thank College of Engineering, King Saud University, Department of Petroleum and Natural Gas Engineering, Department of chemical Engineering, Research Centre at College of Engineering, King Abdullah Institute for Research and Consulting studies for their Support.

References

1. Leverett MC (1941) Capillary Behavior in Porou Solids. Trans AIME 142: 152-69.

2. Brooks RH, Corey AT (1964) Hydraulic Properties of Porous Media. Hydro Paper 3, Colorado State University, Fort Collins.

3. Mualem, YA (1976) A New model for Predicting the Hydraulic Con¬ductivity of Un- Saturated Porous Media. Water Resour Res 12: 513-22.

4. Van Genuchten MT (1980) A Closed Form Equation for Predicting the Hydraulic Conductivity of Unsaturated Soils. Soc Sci Soci Ame J 44: 892-8

5. Oostrom M, Lenhard RJ (1998) Comparison of Relative Permeability. Saturation-Pressure Parametric Models for Infiltration and Redistribu¬tion of a Light Non-Aqueous Phase Liquid in Sandy Porous Media. Adv Water Resour 212: 145-57.

6. Jing XD, VanWunnik JNM (1998) A Capillary Pressure Function for. Interpretation of Core-Scale Displacement Experiments 9807. Impe¬rial College, SCA, UK: 14-22.

7. Li K (2004) Generalized Capillary Pressure and Relative Permeability Model Inferred from Fractal Characterization of Porous Media. In: Pro¬ceedings of the Annual Technical Conference and Exhibition, Houston, Texas, 26-29 September. Society of Petroleum Engineers 89874.

8. Li K, Horne RN (2006) Fractal Modeling of Capillary Pressure Curves for the Geysers Rocks. Geothermic 35: 198-207.

9. Li K (2010a) More General Capillary Pressure and Relative Perme¬ability Models from Fractal Geometry. J Contam Hydrol 111: 13-24.

10. Li K (2010b) Analytical Derivation of Brooks-Corey Type Capillary Pressure Models Using Fractal Geometry and Evaluation of Rock Heterogeneity. J Petr Sci Eng 73: 20-6.

11. Al-Khidir KA, Al-Laboun A, Al-QurishiA, Benzagouta MS (2011) Bi¬modal Pore Size Behavior of the Shajara Formation Reservoirs of the Permo-Carboniferous Unayzah Group, Saudi Arabia. J Pe¬tr Explo Prod Tech 1: 1-9.

12. Al-Khidir K, Benzagouta M, Al-Qurishi A, Al-Laboun A (2013) Charac¬ terization of Heterogeneity of the Shajara Reservoirs of the Shajara Formation of the Permo-Carboniferous Unayzah Group. Arab J Geosci 6: 3989-95.

13. Al-Khidir (2013) Geoscience; New Findings Reported from King Saud University Describe Advances in Geoscience Science Letter (Oct 25, 2013): 359.

14. Al-Khidir KE, Benzagouta MS, Al-Quraishi AA, Al-Laboun AA (2013) Differential Capacity Fractal Dimension and Water Saturation Fractal Dimension as Parameters for Reservoir Characterization: Shajara For¬mation of the Permo-Carboniferous Unayzah Group as a Case Study. 10th Meeting of the Saudi Society for Geoscience Geosciences for Sustainable Development 15-17 April 2013 KFUPM Campus, Dhah¬ran, Saudi Arabia: Monday, April 15, 2013.

15. Al-Khidir (2015) Induced Polarization Relaxation Time Fractal Dimen¬sion Derived from Capillary pressure data for characterizing Shajara Reservoirs of the shajara Formation of the Permo-carboniferous Un¬ayzah Group. The Eleventh International Geological Conference 23 - 25 Rajab 1436 12 - 14 May 2015. Riyadh, Saudi Arabia.

16. Al-khidir KE (2018) Geometric Relaxation Time of Induced Polarization Fractal Dimension for Characterizing Shajara Reservoirs of the Shajara Formation of the Permo-Carboniferous Unayzah Group-Permo. Inter J Petr Res 2: 105-8.